Drought Risk Assessments of Water Resources Systems under Climate Change: A Case Study in Southern Taiwan

T. C. Yang[1], C. Chen[1], C. M. Kuo[1], H. W. Tseng[1] and P. S. Yu[1]

[1]{Department of Hydraulic and Ocean Engineering, National Cheng Kung University, No. 1, University Rd., Tainan 701, Taiwan}

Correspondence to: Professor P. S. Yu (yups@mail.ncku.edu.tw)

Abstract

This study aims at assessing the impact of climate change on drought risk in a water resources system in Southern Taiwan by integrating the weather generator, hydrological model and simulation model of reservoir operation. Three composite indices with multi-aspect measurements of reservoir performance (i.e., reliability, resilience and vulnerability) were compared by their monotonic behaviors to find a suitable one for the study area. The suitable performance index was then validated by the historical drought events and proven to have the capability of being a drought risk index in the study area. The downscaling results under A1B emission scenario from seven general circulation models were used in this work. The projected results show that the average monthly mean inflows during the dry season tend to decrease from the baseline period (1980~1999) to the future period (2020~2039); the average monthly mean inflows during the wet season may increase/decrease in the future. Based on the drought risk index, the analysis results for public and agricultural water uses show that the occurrence frequency of drought may increase and the severity of drought may be more serious during the future period than during the baseline period, which presents a big challenge on water supply and allocation for the authorities of reservoir in Southern Taiwan.

1 Introduction

According to the fourth assessment report of Intergovernmental Panel on Climate Change (IPCC, 2007), most of the observed temperature increase since the middle of the 20th century was caused by increasing concentrations of greenhouse gases. Besides, the occurrence frequency and severity of extreme weather (e.g., droughts and storms) have been considerably raised. The report (IPCC, 2007) also indicates that by the end of the century, climate change will place between 1.1 and 3.2 billion people at risk of water shortages. As we know, water shortages seriously affect the cities' and agricultural communities' social and economic development. Therefore, assessing impacts of climate change on water shortages for water management has become an important world-wide issue recently (Vano et al., 2010; Hall and Murphy, 2010; Schilling et al., 2012; Hanak and Lund, 2012).

In southern Taiwan, Yu et al. (2004, 2006) found that annual rainfall has decreased significantly during the past century. The studies (Tseng et al., 2012; Yu et al., 2004; Yu et al., 2010; Chen et al., 2009) pertaining to impacts of climate change on droughts point out that the occurrence frequency of meteorological and hydrologic droughts, the number of dry days, and the maximum consecutive dry days may increase obviously in the future, which will lead Southern Taiwan have to face possible water shortage and present a big challenge to the managers of the reservoir water supply and allocation.

Tsengwen Reservoir is located in southern Taiwan and the largest water storage facility in Taiwan. The reservoir has to provide an amount of water of about 1,047 million cubic meters (MCM) per year for satisfying all water uses. Nearly 85% of annual rainfall is concentrated in the wet season (from May to October), which makes the wet and dry seasons distinct in the area. Hence, this reservoir plays an important role in providing functions on flood mitigation and water supply in the water resources system. Under climate change, however, the change of hydrological processes in the catchment of reservoir will influence inflows to reservoir. The changes of inflow would further influence reservoir storage, water supply and water shortage. Therefore, assessing the changes of inflow, reservoir storage, water supply and water shortage in the future are essential to the authorities who control the reservoir for adopting suitable adaptation strategies to respond to the impacts of a changing climate.

Besides, in order to assess the impact of climate change on drought risk, a suitable performance index is required which is able to quantify the characteristics of water shortage and be a drought risk index. The notion of drought has several meanings (Mishra and Singh, 2010). For example, meteorological drought (deficit in precipitation), agricultural drought (deficit in soil water), hydrological drought (deficit in river discharge), groundwater drought (deficit in groundwater storage), and socio-economic drought (conflict due to water shortage and water management issues). In our study, drought is the operational drought, that is, a period during which water shortage happens in a water resources system. Indices represent aggregate measures of a combination of performance measures. Several indices have been developed specifically for water resources, such as the drought risk index (*DRI*) (Zongxue et al., 1998), the Palmer drought severity index (Palmer, 1965), water quality index (Brown et al., 1972), fairness (Lence et al., 1997), reversibility (Fanai and Burn, 1997), and consensus (Takeuchi et al., 1998). To quantify the sustainability of water resources systems, Loucks (1997) proposed the sustainability index (*SUI*), with the objective to facilitate the evaluation and comparison of water management policies. The *SUI* has been used by many researchers (Sandoval-Solis et al., 2011; Ray et al., 2010; McMahon et al., 2006; Loucks, 1997). The *DRI* and *SUI* summarize essential performance parameters of water management in a meaningful manner (i.e., reliability, resilience and vulnerability) and can be used to be drought risk indices to quantify the characteristics of water shortage in a water resources system. In our study, three indices (i.e., *DRI*, *SUI* and a modified *SUI*) were adopted. Performances of these three indices were compared by their monotonic behaviors to find a suitable one for the study area.

This study aims to find a suitable drought risk index which is capable of multi-aspect description of water shortage (including duration, number and severity) and assess the impact of climate change on reservoir inflow, reservoir storage, water supply and water shortage in the water resources system. The rest part of this paper is organized as follows. Section 2 "Study area and data set" provides a summary description of the study area and the data set. Section 3 "Methodologies" lists the models and indices which comprise weather generator, hydrological model, simulation model of reservoir operation and performance indices of water resources system (including single and composite indices). Section 4 "Analysis results" makes calibration and validation of hydrological model in the reservoir catchment in Section 4.1; comparisons of composite index in Section 4.2 to find the most suitable one; drought classification by the most suitable index and validation by historical events in Section 4.3 to test the index's ability; and impact assessment of climate change on reservoir inflow, reservoir storage, water supply and drought risk in Section 4.4. Finally, Section 5 "Conclusions" concludes the paper and gives some future work.

2 Study Area and Data Set

Tsengwen Reservoir, completed in 1973 with a storage capacity of about 780 MCM, is the largest reservoir in Taiwan and has multifunction of water supplies for agricultural water use, industrial water use, public water use, flood control and hydropower generation. The reservoir has to provide an amount of water of about 1,047 MCM per year (i.e., the average demand) for satisfying all water uses. The catchment area of Tsengwen Reservoir is about 481 km^2 and is at an elevation of from 157 to 3,514 m above sea level. The locations of the study area, the reservoir and the raingauges are displayed in Fig. 1(a). For this area, the mean annual precipitation is about 2,740 mm/year, of which 85% occurs during the wet season (from May to October) as shown in Fig. 1(b).

Daily hydrological data, including rainfall, streamflow and temperature, continuously from 1975 to 2008 were used as the data set. The daily streamflow data are the inflow of Tsengwen Reservoir. The daily rainfall data were collected from the nine raingauges from which areal precipitations on the reservoir catchment were computed using the Thiessen polygon method. The daily mean temperature data were collected from two meteorological stations (i.e., Tsengwen and A-Li-Shan stations) from which the two stations' daily data in a day were averaged as the representative temperature of the reservoir catchment.

In the study, the future period is set to 2020~2039 and the baseline period is set to 1980~1999. Taiwan Climate Change Projection and Information Platform Project (TCCIP) (National Science Council of Taiwan, 2010) provides the downscaling projections of monthly rainfall and monthly mean temperature from the 24 general circulation models (GCMs) for each node of a 25km×25km grid (covering Taiwan) under A1B, B1, and A2 emission scenarios. Besides, for each GCM, each grid node and each month, the change rates (%) of monthly rainfall and the changes (^{o}C) of monthly mean temperature from the baseline period to the future period are also provided. Seven GCMs that are reported to properly consider the tropical cyclone information and East Asian Monsoon modeling, as mentioned in the study of Chu and Yu (2010), were used in this work. Table 1 gives the information about seven used GCMs in this study. The seven GCMs include CGCM3.1(T63), CSIRO-Mk3.5, ECHAM5/MPI-OM, GFDL-CM2.0, GFDL-CM2.1, MIROC3.2(hires), and MRI-CGCM2.3.2. In the study, only the A1B emission scenario was chosen. The change rates (%) of monthly rainfall and the changes (^{o}C) of monthly mean temperature from the baseline period to the future period for these seven GCMs are listed in Table 2 and Table 3, respectively.

The change rates (%) in Table 2 are the shifts in mean monthly rainfalls from the baseline period (1980~1999) to the future period (2020~2039) under A1B emission scenario. They are subject to different GCMs and months. Overall, the change rates (%) vary from -55.42 to 57.34. The changes (^{o}C) in Table 3 are the shifts in monthly mean temperatures from the baseline period from the baseline period (1980~1999) to the future period (2020~2039) under A1B emission scenario. They are also subject to different GCMs and months. The changes (^{o}C) vary from 0.22 to 1.70. All the seven GCMs reveal a consistent projection of increased temperature in the future.

3 Methodologies

3.1 Weather Generator

The daily precipitation generation is based on procedures proposed by Richardson (1981). The generator uses a Markov chain to model the occurrence of wet or dry days, and then uses a probability distribution to generate the precipitation amount conditional on a wet day modeled by the Markov chain. A first-order two-state Markov chain was used in this work. The occurrence of a dry or wet day is modeled by a transition probability matrix consisting of conditional probabilities, given a previous dry or wet day.

Many probability distributions were applied to generate daily precipitation amount, such as the exponential distribution (Selker et al., 1990; Tung et al., 1995), Weibull distribution (Yu et al., 2002), two-parameter gamma distribution (Richardson, 1981; Coe et al., 1982; Woolhiser et al., 1982; Schubert, 1994; Corte-Real et al., 1999), and mixed exponential distribution (Woolhiser et al., 1979; Woolhiser et al., 1982, 1986). Among the probability distributions, the Weibull distribution most appropriately approximates daily rainfall in Taiwan (Yu et al., 2002); consequently, this work used the Weibull distribution to generate daily rainfall.

Regarding the daily temperature generation, a first-order autoregressive model was utilized to generate the daily temperature sequences in each month. This daily temperature generation model is expressed as follows:

$$T_k = \mu_T + \rho_{1T}\left(T_{k-1} - \mu_T\right) + \sqrt{1-\rho_{1T}^2}\,\sigma_T v_k + \Delta\mu \quad (1)$$

where T_k is the temperature (°C) on day k; μ_T is the mean temperature (°C) in a certain month; σ_T is the standard deviation of daily temperature (°C) in the month; ρ_{1T} is the lag-1 autocorrelation coefficient of daily temperature in the month; ν_k is the random standard normal variate, and $\Delta\mu$ is the mean temperature change (°C) in the month under a future scenario. Given the parameters, μ_T, σ_T, ρ_{1T}, and $\Delta\mu$, a daily temperature sequence in a month can be generated by this model.

3.2 Hydrological Model

A continuous hydrologic model was used to simulate future projected streamflow, after the daily precipitation and temperature were obtained in the previous section by the downscaling method. This work used a continuous hydrologic model based on the structure of HBV hydrological model (Bergström, 1976, 1992), which was initially designed for use in Scandinavian catchments by the Swedish meteorological and hydrological institute. Yu and Yang (2000) adapted the HBV hydrological model structure to suit catchments in Taiwan. The HBV-based hydrological model uses both an upper and lower tanks to model the rainfall-runoff behavior. Model structure mainly consists of three parts: (1) soil moisture module, (2) runoff response mechanism, and (3) water balance functions. Detail description of the HBV-based hydrological model, as well as its procedures for calibration and validation in this work, can be found in Yu and Yang (2000) and Yu *et al.* (2002).

In the HBV-based hydrological model, Hamon's temperature-dependent equation (Hamon, 1961) was used to transform the daily temperature series into the daily potential evapotranspirartion series. The Hamon's temperature-dependent equation is as:

$$Ep_t = 0.21 H_t^{\,2} e_t / [T_t + 273] \qquad (2)$$

where Ep_t is the potential evapotranspiration (mm/day) on day t; H_t is the sunshine duration (hour) on day t. The sunshine duration can be decided from the observed data at the nearby meteorological station (i.e., A-Li-Shan station); e_t is the saturated vapor pressure (hPa) on day t; T_t is the mean temperature (°C) on day t. The value of e_t can be estimated by the following empirical equation:

$$e_t = 33.8639 \times [(0.00738 T_t + 0.8072)^8 - 0.000019 \times |1.8 T_t + 48| + 0.001316] \qquad (3)$$

Once the potential evapotranspiration is estimated by the Hamon's equation, a relationshop between soil moisture and potential evapotranspiration is applied to calculate the actual evapotranspiration (more details can be found in Yu *et al.*, 2002).

3.3 Simulation Model of Reservoir Operation

The daily inflow time series are routed through a reservoir system for simulating water supply process. The reservoir system can be described by the following continuity equation. While the hydropower generation uses and releases water instantaneously but does not consume water, only water supply and flood control are considered in reservoir operation. The equation includes the inflow, draft (water supply), evaporation, spill (flood control) and storage of reservoir in each time period.

$$S_{t+1} = S_t + I_t - O_t - E_t \tag{4}$$

$$S_{t+1} = \begin{cases} S_{\max} & ;Q_t^{over} = S_{t+1} - S_{\max} \quad ;if \quad S_{t+1} > S_{\max} \\ S_{t+1} & ;Q_t^{over} = 0 \quad ;if \quad S_{t+1} \le S_{\max} \end{cases} \tag{5}$$

where S_{t+1} is the storage of reservoir (MCM) on day t+1; S_t is the storage of reservoir (MCM) on day t ; I_t and E_t represent inflow (MCM) and evaporation loss (MCM) for the reservoir on day t. The evaporation loss (MCM) from the reservoir is defined by the area of water surface times the evaporation per unit area of water surface and the value of evaporation per unit area of water surface can be obtained from the observed data of evaporation pan at the nearby meteorological station (i.e., Tsengwen station); S_t is the storage of reservoir (MCM) on day t which can vary from 0 to S_{max} (i.e., storage capacity); O_t is the draft (MCM) from the reservoir for different water uses (i.e., $O_t = DO_t + IAO_t$) on day t; Q_t^{over} is the spill (MCM) on day t; $S_{\max}$ is the storage capacity of reservoir (MCM); DO_t is the draft (MCM) for domestic water use on day t; IAO_t is the draft (MCM) for industrial and agricultural water uses on day t.

The drafts from Tsengwen Reservoir are decided by the reservoir storage and the operation rule curves (Fig. 2). The drafts for domestic water use (DO_t) and industrial and agricultural water uses (IAO_t) are based on the following rules:

$$DO_t = DD_t ,\ IAO_t = IAD_t ;\ \text{if}\ S_t > L_{upper} \tag{6}$$

$$DO_t = DD_t,\ IAO_t = IAD_t;\ \text{if } L_{upper} > S_t > L_{middle} \tag{7}$$

$$DO_t = A_1 \times DD_t,\ IAO_t = A_2 \times IAD_t;\ \text{if } L_{middle} > S_t > L_{lower} \tag{8}$$

$$DO_t = B_1 \times DD_t,\ IAO_t = B_2 \times IAD_t;\ \text{if } L_{lower} > S_t > S_{min} \tag{9}$$

$$DO_t = IAD_t = 0,\ \text{if } S_{min} > S_t \tag{10}$$

where DO_t is the draft (MCM) for domestic water use on day t; DD_t is the demand (MCM) for domestic water use on day t; IAO_t is the draft (MCM) for industrial and agricultural water uses on day t; IAD_t is the demand (MCM) for industrial and agricultural water uses on day t; S_t is the reservoir storage (MCM) on day t; L_{upper} is the upper limit of rule curve (MCM); L_{middle} is the middle limit of rule curve (MCM); L_{lower} is the lower limit of rule curve (MCM); S_{min} is the dead storage of reservoir (MCM); A_1 is the rate of discount for public water use when $L_{middle} > S_t > L_{lower}$; A_2 is the rate of discount for agricultural and industrial water uses when $L_{middle} > S_t > L_{lower}$; B_1 is the rate of discount for public water use when $L_{lower} > S_t$; B_2 is the rate of discount for agricultural and industrial water uses when $L_{lower} > S_t$. These rates of discount are used to reduce the amount of water supply for more water reservation when the reservoir storage is below the limit of operation rule curve. Referring to "Operation Directions for Tsengwen Reservoir", the values of A1, A2, B1 and B2 are 1.00, 0.75, 0.80 and 0.50, respectively.

Figure 3 shows demands of agricultural, industrial, and domestic water uses. These demands will be fully supplied when the water of reservoir is abundant. Otherwise, the supplies will be reduced when the water of reservoir is scarce.

3.4 Performance Indices of Water Resources System

3.4.1 Single indices

Generally, failures in the operation of a reservoir have many aspects: extent, number, severity (Jain, 2010). In the following, the single indices (i.e., reliability, resilience and vulnerability) which are used to measure different aspects of the performance of a reservoir are described. Usually these single indices are computed using daily, monthly or annual data for the operation of the system. In the study, the daily data were used. The following description of the single indices is based on the assumption that the system under consideration at a given time t can be in either a satisfactory (i.e. non-failure, NF) state or an unsatisfactory (i.e. failure, *F*) state. In this study, the focus is on water resources systems. Therefore, the *NF* state occurs when water supply is able to meet water demand and, hence, the *F* state is when supply cannot meet demand.

a. Reliability

Water supply reliability is the probability that the available water supply meets the water demand during the period of simulation (Klemes et al. 1981; Hashimoto et al. 1982). For each time period t, deficit D_t is positive when the water demand X_{D_t} is more than the water supply X_{S_t}; if the water supply is equal to water demand ($X_{D_t} = X_{S_t}$), deficit is zero (D_t=0) (Loucks 1997).

$$D_t = \begin{cases} X_{D_t} - X_{S_t} & if \quad X_{D_t} > X_{S_t} \\ 0 & if \quad X_{D_t} = X_{S_t} \end{cases} \tag{11}$$

The most widely accepted and applied definition for water resources systems is occurrence reliability (Hashimoto et al. 1982), which is the portion of time that the water demand is fully supplied (i.e. non-failure state, *NF*) and can be estimated as:

$$Rel = 1 - \frac{No. of\ days\ D_t > 0}{n} \tag{12}$$

where D_t is water deficit on day t and n is the total number of time intervals (days).

b. Resilience

Resilience (*Res*) is a measure of how fast a system is likely to return to a satisfactory state (i.e., *NF* state) once the system has entered an unsatisfactory state (i.e., *F* state). Hashimoto et al. (1982) define resilience as a conditional probability:

$$Res = \frac{P\{S_t \in NF, S_{t-1} \in F\}}{P\{S_t \in F\}} \tag{13}$$

where S_t is the system state variable under consideration. Moy et al. (1986) used the maximum number of consecutive deficit periods prior to recovery as an alternative definition of resilience. Resilience is the probability that a successful period follows a failure period (the number of times D_t = 0 follows D_t > 0) for all failure periods (the number of times D_t > 0 occurred). This statistic assesses the recovery of the system once it has failed:

$$Res = \frac{No.\ of\ \ days\ D_t =\ 0\ following\ \ the\ period\ \ D_t >\ 0}{No.\ of\ \ days\ D_t >\ 0\ occurred} \tag{14}$$

where D_t is water deficit on day t.

c. Vulnerability

Vulnerability expresses the severity of failures. Vulnerability can be expressed as (1) the average failure (Loucks and van Beek 2005; Sandoval-Solis et al., 2011); (2) the average of maximum shortfalls over all continuous failure periods (Hashimoto et al. 1982; McMahon et al. 2006); and (3) the probability of exceeding a certain deficit threshold (Mendoza et al. 1997). This paper uses the first approach, the expected value of deficits, which is the sum of the deficits, D_t , divided by the deficit period, the number of times (days) $D_t > 0$ occurred. Dimensionless vulnerability is calculated by dividing the average daily deficit by the average daily water demand (WD):

$$Vul = \frac{\left(\sum_{t=0}^{t=n} D_t\right) \Big/ No.\ of\ \ days\ D_t >\ 0\ occurred}{WD} \tag{15}$$

where D_t is water deficit on day t and n is the total number of time intervals (days); WD is the average daily water demand.

3.4.2 Composite indices

The single indices (i.e., reliability, resilience and vulnerability) which are used to measure different aspects of the performance of a reservoir. Reliability, resilience and vulnerability imply the extent, number, and severity of water shortage events. In the recent past, some attempts (Loucks, 1997; Zongxue et al., 1998) have been made to quantitatively represent sustainability of water resources managements by using the composite indices which are composed of the three single indices. Composite indices are more efficient than single indices which can measure various characteristics of drought event.

Zongxue et al. (1998) proposed an integrated risk index, drought risk index (DRI), as a linear weighted function of reliability and resiliency and vulnerability.

$$DRI = \frac{1}{3}(1 - Rel) + \frac{1}{3}(1 - Res) + \frac{1}{3}Vul \tag{16}$$

where Rel is reliability; Res is resilience; Vul is vulnerability. The DRI's values vary from 0~1 and the value closer to 1 means the condition of water shortage is more serious.

Loucks (1997) proposed the sustainability index (*SUI*), which has the following properties: (1) its values vary from 0~1; (2) if one of the performance criteria is zero, the sustainability will be zero also; and (3) there is an implicit weighting because the index gives added weight to the criteria with the worst performance. The multiplicative form of the index considers each criterion as essential and nonsubstitutable. The *SUI* summarizes essential performance parameters of water management in a meaningful manner and the *SUI* has been used by the scientific community (Sandoval-Solis et al., 2011; Ray et al., 2010; McMahon et al., 2006; Loucks ,1997)

$$SUI = \left[Rel \times Res \times (1 - Vul) \right]^{\frac{1}{3}} \tag{17}$$

where *Rel* is reliability; *Res* is resilience; *Vul* is vulnerability. *SUI*'s values vary from 0~1 and the value closer to 1 means the condition of water shortage is less serious. The study slightly modified the *SUI* into the following form (called *MSUI*) whose values vary from 0~1. As *DRI*, the *MSUI*'s value closer to 1 means the condition of water shortage is more serious.

$$MSUI = \left[(1 - Rel) \times (1 - Res) \times Vul \right]^{\frac{1}{3}} \tag{18}$$

where *Rel* is reliability; *Res* is resilience; *Vul* is vulnerability. The study uses the three composite indices, including *DRI*, *SUI* and *MSUI*, for behavior analysis to choose a suitable one as the drought risk index for the study area. Although the composite indices can simultaneously measure different characteristics of drought event, the complementary relation between single indices should be noticed and checked before one uses the aforementioned composite indices. For example, McMahon et al. (2006) have found that vulnerability is an approximate complement of resilience in their study.

4 Analysis Results

4.1 Performance of Weather Generator

For inspecting the performance of weather generator in reproducing the statistics of observed weather data, the statistics of mean, standard deviation and skewness for the observed and generated daily rainfalls and temperatures were calculated and compared in Table 4. The observed weather data used herein are during the baseline period (1980~1999). The results in Table 4 show that the mean and standard deviation of daily rainfalls and daily temperatures for each month are well preserved. Though the Weibull distribution and the first-order autoregressive model do not include the parameter of skewness, the values of skewness of daily rainfall and daily temperature seem to be preserved. It is found that the positive skewness exits in daily rainfalls and the approximate zero skewness exists in daily temperatures. The evaluation results show that weather generator performs reasonably at daily scale for each month.

When generating daily rainfalls for a water resource system, preserving the statistics of rainfall in longer periods (e.g., month and year) is very essential. The study further evaluated the performance of weather generator at longer time scales. Table 5 shows the comparison of statistics for observed and generated rainfalls at both monthly and yearly scales. The results also show that the mean and standard deviation of monthly and yearly rainfalls are reasonably preserved. The positive skewness exists in monthly and yearly rainfalls, and the skewness values of observed and generated rainfalls seem to be close. Overall, the daily generated rainfalls preserve the monthly and annual time series characteristics of mean, standard deviation and skewness. Moreover, the lag-1 autocorrelation coefficients for observed and generated rainfalls at monthly and yearly scales were calculated. The lag-1 autocorrelation coefficients for monthly observed and generated rainfalls are 0.44 and 0.66, respectively. It reveals that both the values of lag-1 autocorrelation (*r*) belong to moderate correlation (i.e., $0.3 \le |r| \le 0.7$). The lag-1 autocorrelation coefficients for yearly observed and generated rainfalls are -0.25 and 0.01, respectively. It reveals that both the values of lag-1 autocorrelation belong to week correlation (i.e., $|r| \le 0.3$). The aforementioned results show that the daily generated rainfalls roughly preserve the autocorrelation of monthly and annual time series.

4.2 Calibration and Validation of HBV-based Hydrological Model

The HBV-based hydrological model was applied in the catchment of Tsengwen Reservoir for inflow simulation. The fuzzy multiple objective functions, proposed by Yu and Yang (2000), and the shuffled complex evolution optimization method (Duan et al., 1994) were adopted in the study. Historical daily rainfall, temperature, and inflow data from 1975 to 2000 were used for model calibration. The calibrated HBV-based hydrological model was further verified by historical data from 2001 to 2008. To assess the model performance, three criteria, including the ratio of the summation of simulated inflows to the summation of observed inflows (*Ratio*), the root mean squared error (*RMSE*), and the coefficient of correlation (*CC*) between simulated and observed daily inflows, were calculated for the calibration and verification periods, respectively. During the calibration period, the values of *Ratio*, *RMSE* and *CC* are 0.957, 6.849 (mm) and 0.938, respectively. During the validation period, the values of *Ratio*, *RMSE* and *CC* are 0.985, 9.539 (mm) and 0.964, respectively. Figures 4(a) and 4(b) show the calibration and verification results in 1976 and 2002, respectively. These results reveal the HBV-based hydrological model is able to simulate the rainfall-runoff behavior over the study area.

4.3 Comparisons of Composite Index

According to the researches (Jain, 2010; Kjeldsen and Rosbjerg, 2004), the water resource indices should have monotonic behaviors. The study investigated the degree of monotonic behavior of the three composite indices (*DRI*, *SUI*, and *MSUI*) for choosing a suitable one for the water resource system in the study area. The observed inflows have been used for analysis of monotonic behavior by estimating the three composite indices with changes in (1) evaporation, (2) water demand, (3) reservoir storage capacity and (4) reservoir inflow.

The analysis results of monotonic behavior for each index are shown in Fig. 5. The estimates of *DRI* exhibit monotonic behaviors in Fig. 5(a) as the water demand, reservoir storage capacity and reservoir inflow increase. However, the estimates of *DRI* exhibit a non-monotonic decrease as the evaporation increases in Fig. 5(a). In Fig. 5(b), the estimates of *SUI* generally exhibit non-monotonic behaviors as the estimates do not increase or decrease monotonously as the evaporation, water demand, reservoir storage capacity and reservoir inflow increase. In Fig. 5(c), the estimates of *MSUI* exhibit monotonic behaviors as the estimates increase or decrease monotonously as the evaporation, water demand, reservoir storage capacity and reservoir inflow increase. Based on the above comparisons of monotonic behavior, *MSUI* performed the best and was chosen as the suitable index for the following analysis in the study area.

4.4 Drought Classification by *MSUI* and Validation by Historical Events

In order to classify the level of drought by *MSUI*, determining different thresholds of *MSUI* for different degrees of drought is necessary. The study refers to the drought classification standard, proposed by Water Resource Agency (WRA), Taiwan, for determining the thresholds of *MSUI* for different levels of drought. The drought classification standard of

WRA is based on the deficit rates for public and agricultural water supplies. Here, the public water supply is defined as the sum of domestic and industrial water supplies. According to the standard of WRA, three intervals of deficit rate for public water supply, >30%, 20~30% and 10~20%, are defined as Level 1, Level 2 and Level 3, respectively; three intervals of deficit rate for agricultural water supply, >50%, 40~50% and 30~40%, are defined as Level 1, Level 2, Level 3. Moreover, the operation of Tsengwen Reservoir is based on a 10-day period. The water supplies from the reservoir are decided every 10-day period on the basis of operation rule curves. Hence, this work uses the time scale, 10-day period, for following calculation.

The value of *MSUI*, public and agricultural deficit rates for each 10-day period were computed from 1981 to 1999. For each drought level, the values of *MSUI* are displayed by using the box plot in Fig. 6(a) and Fig. 6(b) for public and agricultural water supplies, respectively. For each drought level, the median of *MSUI* value was used to determine the intervals of *MSUI* value for different drought levels as follows. For the public water supply system, the *MSUI* value of 0.8~1.0 is classified into Level 1; the *MSUI* value of 0.5~0.8 is classified into Level 2; and the *MSUI* value of 0.4~0.5 is classified into Level 3. For the agricultural water supply system, three intervals of *MSUI* value (i.e., 0.9~1.0, 0.8~0.9 and 0.7~0.8) were classified into Level 1, Level 2 and Level 3, respectively. Drought levels and their corresponding *MSUI* values and deficit rates are shown in Fig. 7.

In order to validate whether *MSUI* can judge drought event or not, the study used two periods (1981~1999 and 2000~2007) of historical drought events for validating and testing the *MSUI*'s performances, respectively. During the historical drought periods, the percentage, p_x, of the 10-day number with $MSUI \geq x$ to the 10-day number of historical drought was calculated as

$$p_x = \frac{N_{(MSUI \geq x \mid HD)}}{N_{HD}} \tag{19}$$

where x is a threshold of *MSUI*, *HD* means historical drought period, N_{HD} indicates the 10-day number of historical drought, and $N_{(MSUI \geq x \mid HD)}$ denotes the 10-day number with $MSUI \geq x$ during the historical drought periods.

The results during the validating period (1981~1999) are shown in Fig. 8. From the figure, when the threshold of *MSUI* (x) is less than or equal to 0.4, the percentage (p_x) is the highest (i.e., $p_{0.1}$=$p_{0.2}$= $p_{0.3}$=$p_{0.4}$=79.12%). While, when the threshold of *MSUI* (x) is greater than 0.4, the percentage (p_x) decreases, which means that 0.4 is a threshold value of *MSUI* for catching most of the historical drought events. Moreover, the value of 0.4 is the same as the threshold of Drought Level 3 for public water supply system, which implies that the value of 0.4 is a reasonable threshold for the lowest level of drought. Further, the percentage for *MSUI* $\geq$ 0.4 (i.e., $p_{0.4}$) during the testing period (2000~2007) is 93.0%, which also reveals that *MSUI* is effective as the indicator of drought risk assessment and used to determine the severity of water shortage and occurrence of drought event.

4.5 Impact Assessment of Climate Change

4.5.1 Impact on Rainfall, Temperature and Reservoir Inflow

The downscaling results provided by TCCIP in Table 2 and Table 3 are considered as the adjustment factors for rainfall and temperature generation, respectively. Using the change rates of monthly rainfall in Table 2 and the changes of monthly mean temperature in Table 3**,** the parameters in the weather generator (i.e., mean of Weibull distribution and μ_T in Eq. (1)) have been adjusted for future rainfall and temperature generation. For example, in Table 2, each change rate of monthly rainfall plus one is taken as the change ratio. Then, the historical monthly mean rainfalls multiplied by the corresponding change ratios are the adjusted parameters (i.e., mean of Weibull distribution) used for future rainfall generation. The historical monthly mean temperatures plus the corresponding changes are regarded as the adjusted parameters (i.e., μ_T in Eq. (1)) used for future temperature generation.

For each generation, 200 years of daily rainfall/temperature are synthesized as projected scenario data. Then, these projected scenario data will be further compared with baseline data. The baseline data are also generated by weather generator but without consideration of climate change (the parameters in the weather generator are not be adjusted). The projected mean monthly rainfalls by different GCMs under A1B emission scenario are shown in Fig. 9(a). The ensemble is derived by averaging the results of seven GCMs for showing the average property of various GCMs. The projected rainfall amounts by different GCMs vary from 318 mm to 388 mm during the dry season and from 1,840 mm to 2,408 mm during the wet season. The baseline rainfall amounts during the dry and wet seasons are 381 mm and 2,167 mm, respectively. The results show that the rainfall amount during the dry season tends to decrease from the baseline period to the future period; while, the rainfall amount during the wet season has an uncertain trend which may increase or decrease from the baseline period to the future period. The projected average monthly mean temperatures by different GCMs under A1B emission scenario are shown in Fig. 9(b), which reveals the increases of projected average monthly mean temperatures by different GCMs in spring and winter are larger than in summer and autumn.

By using the above projected rainfalls and temperatures as input, the HBV-based hydrological model was performed to generate the reservoir inflows. Figure 9(c) shows the average monthly mean inflows during the baseline period and the future period. During the baseline period, the average monthly mean inflows during the dry and wet seasons are 6.01 m^3/s and 53.70 m^3/s, respectively. The projected average monthly mean inflows by different GCMs vary from 3.34 m^3/s to 5.47 m^3/s during the dry season and from 43.80 m^3/s to 59.50 m^3/s during the wet season. The results show that the average monthly mean inflows during the dry season tend to decrease from the baseline period to the future period; while, the average monthly mean inflows during the wet season have an uncertain trend which may increase or decrease from the baseline period to the future period.

4.5.2 Impact on Reservoir Storage and Water Supply

Through the weather generator and the HBV-based hydrological model, the simulated inflows of reservoir have system errors resulted from uncertainties of model structure and parameters. In order to reduce system errors and keep the generated inflow temporal pattern close to the observed inflow temporal pattern, the study used the observed daily inflows during the baseline period (1980~1999) and the adjusted daily inflows during the future period (2020~2039) for simulation of reservoir system to investigate impacts of climate change on reservoir storage, water supply and drought risk. The adjusted daily inflows during the future period were obtained by the adjusting factor as

$$C_{S_i} = \frac{Q_{S_i}}{Q_{B_i}} \tag{20}$$

where C_{S_i} is the adjusting factor for the i^{th} month; Q_{S_i} is the generated mean monthly inflow in the i^{th} month during the future period; Q_{B_i} is the generated mean monthly inflow in the i^{th} month during the baseline period by using the weather generator and the HBV-based hydrological model. The adjusted daily inflows during the future period were obtained by using the observed daily inflows multiplied by the adjusting factor.

$$Q_{A_{i,j}} = Q_{O_{i,j}} \times C_{S_i} \quad (21)$$

where $Q_{A_{i,j}}$ is the adjusted daily inflows on the j^{th} day in the i^{th} month during the future period; $Q_{O_{i,j}}$ is the observed daily inflows on the j^{th} day in the i^{th} month during the baseline period; C_{S_i} is the adjusting factor for the i^{th} month.

Through the simulation of reservoir operation, the mean monthly storages and water supply amounts during the baseline period and during the future period, respectively, were calculated. The percentage changes of mean monthly storage and mean monthly water supply amount from the baseline period to the future period are shown in Fig. 10 and Fig. 11, respectively. The figures reveal the decreases of storage and water supply amount are larger in April to June than in the other months. In May, the percentage change of storage ranges from -1.2% to -37.8% and the percentage change of water supply amount ranges from -0.3% to -13.3%.

4.5.3 Impact on Drought Risk

The values of *MSUI* for each 10-day period during the baseline and future periods were computed for public and agricultural water supply-demand systems, respectively. These values of *MSUI* for each 10-day period were then classified into different drought levels by using the intervals for different drought levels in Fig. 7. Figure 12(a) shows the numbers of 10-day period of different drought levels for public water supply-demand system during the baseline and future periods. In the figure, the numbers of 10-day period are 19 for Drought Level 1, 134 for Drought Level 2, and 16 for Drought Level 3 during the baseline period. By comparing the numbers of 10-day period for different drought levels during the baseline period and the future period under A1B emission scenario, the following results can be found: (1) the number of 10-day period for Drought Level 2 increases a lot and is around 2.34 times of the number of 10-day period during the baseline period; (2) the total number of 10-day period (for Drought Levels 1, 2, and 3) is around 2.2 times of the total number of 10-day period during the baseline period. The aforementioned finding reveals that the number of 10-day period which satisfies the public water demand seems to decrease under the A1B emission scenario, which implies that the drought risk for public water use will rise in the future.

Figure 12(b) shows the numbers of 10-day period of different drought levels for agricultural water supply-demand system during the baseline and future periods. In the figure, the numbers of 10-day period are 14 for Drought Level 1, 5 for Drought Level 2, and 85 for Drought Level 3 during the baseline period. By comparing the numbers of 10-day period for different drought levels during the baseline period and the future period under A1B emission scenario, the following results can be found: (1) the number of 10-day period for Drought Level 3 increases a lot and is around 1.81 times of the numbers of 10-day period during the baseline period; (2) the total number of 10-day period (for Drought Levels 1, 2, and 3) is around 1.8 times of the total number of 10-day period during the baseline period. The aforementioned finding reveals that the number of 10-day period which satisfies the agricultural water demand seems to decrease under the A1B emission scenario, which implies that the drought risk for agricultural water use will rise in the future.

The above drought risk assessment reveals that the occurrence frequency of drought may increase and the severity of drought may be more serious during the future period than during the baseline period, which presents a big challenge on water supply and allocation for the authorities of reservoir in Southern Taiwan.

5 Conclusions

This study assessed the impact of climate change on the drought risk in a water resources system in Southern Taiwan. By integrating the weather generator, hydrological model, and reservoir system model, the reservoir inflows and drafts under the climate change scenario were generated. Through the performance index of water resources system, the impact of climate change on the drought risk was assessed.

Apart from previous studies using the shortage rate as the level of water shortage hazard, this study used three composite indices with multi-aspect description of water shortage, including duration, number and severity of water shortage. Composite indices are more efficient than single indices which can measure various characteristic of drought event. This kind of composite index can provide more information about drought events. Three composite performance indices (*DRI*, *SUI*, and *MSUI*) were compared by their monotonic behaviors to find a suitable one for the study area to assess the impact of climate change on the risk of water shortage. Each composite index is composed of three single indices (i.e., reliability, resilience and vulnerability) which are used to measure different aspects (i.e., the extent, number, and severity) of water shortage events. The *MSUI* was found to have monotonic behaviors with changes in (1) evaporation, (2) water demand, (3) reservoir storage capacity and (4) reservoir inflow, and be the most suitable one for the study area. The *MSUI* was then validated by the historical drought events and proven to have the capability of being the criterion of drought in the study area. Moreover, enhencing the link between composite indices and practical applications is very essential. In Taiwan, the present drought classification standard, proposed by WRA (Taiwan), considers only a varible (i.e., the deficit rate) for drought classification. Using composite indices (e.g., *MSUI*) as drought classification variables, which can measure different aspects of water shortage events, will be an important issue and the future work.

The downscaling results under A1B emission scenario from seven GCMs that consider the tropical cyclone information and East Asian Monsoon modeling were used in this work. The inflow projected results show that the average discharges during the dry season tends to decrease from the baseline period (1980~1999) to the future period (2020~2039); the average discharge during the wet season may increase/decrease from the baseline period to the future period.

From the analysis results of drought risk for public and agricultural water uses under A1B emission scenario, the total numbers of 10-day period for all drought levels are around 2.20 and 1.80 times of the total numbers of 10-day period during the baseline period, respectively. The results indicate the occurrence frequency of drought may increase and the severity of drought may be more serious during the future period than during the baseline period, which presents a big challenge on water supply and allocation for the authorities of reservoir in Southern Taiwan.

Because the study aims at assessing the climate change impacts on water supply and subsequent drought risk, the assumption of no change in operation modes during both the baseline period and the future period has been made. Therefore, the study let the reservoir be operated with fixed rule curves and fixed reduction factors for this assumption. For reducing the impacts under climate change, optimization for reservoir operation is an efficient approach and will be considered as the future work.

Acknowledgements

The authors would like to thank the National Science Council of the Republic of China (Taiwan) for financially supporting this research under Contract No. NSC 97-2221-E-006-

150-MY3 and Taiwan Climate Change Projection and Information Platform Project (TCCIP) for offering future precipitation projections.

References

Bergström, S.: Development and application of a conceptual runoff model for Scandinavian Catchments, SMHI, Reports RHO. 7, Norrköping, 1976.

Bergström, S.: The HBV model - its structure and applications, SMHI, Reports RHO. 4, Norrköping, 1992.

Brown, R. M., McClelland, N. I., Deininger, R. A., and O'Connor, M. F.: A water quality index - Crashing the psychological barrier, Indicators of environmental quality, Plenum, New York, 1972.

Chen, S. T., Kuo, C. C., and Yu, P. S.: Historical trends and variability of meteorological droughts in Taiwan, Hydrological Sciences Journal, 54, 430-441, 2009.

Chu, J. L., and Yu, P. S.: A study of the impact of climate change on local precipitation using statistical downscaling, Journal of Geophysical Research, 115, D10105, 2010.

Coe, R., and Stern, R. D.: Fitting models to rainfall data, Journal of Applied Meteorology, 21, 1024-1031, 1982.

Corte-Real, J., Xu, H., and Qian, B.: A weather generator for obtaining daily precipitation scenarios based on circulation patterns, Climate Research, 13, 61-75, 1999.

Duan, Q., Sorooshian, S., and Gupta, V. K.: Optimal use of the SCE-UA global optimisation method for calibrating watershed models, Journal of Hydrology, 158, 265-284, 1994.

Fanai, N., and Burn, D. H.: Reversibility as a sustainability criterion for project selection, International Journal of Sustainable Development and World Ecology, 4, 259-273, 1997.

Hall, J., and Murphy, C.: Vulnerability analysis of future public water supply under changing climate conditions: A study of the Moy catchment, Western Ireland, Water Resources Management, 24, 3527-3545, 2010.

Hamon, W. R.: Estimating potential evapotranspiration, Journal of Hydraulics Division, Proceedings of the American Society of Civil Engineers, 871, 107-120, 1961.

Hanak, E., and Lund, J. R.: Adapting California's water mangement to climate change, Climatic Change, 111, 17-44, 2012.

Hashimoto, T., Stedinger, J. R., and Loucks, D. P.: Reliability, resiliency, and vulnerability criteria for water-resource system performance evaluation, Water Resources Research, 18, 14-20, 1982.

IPCC: Climate change 2007: the physical science basis, The Fourth Assessment Report, 2007.

Jain, S. K.: Investigating the behavior of statistical indices for performance assessment of a reservoir, Journal of Hydrology, 391, 90-96, 2010.

Kjeldsen, T. R., and Rosbjerg, D.: Choice of reliability, resilience and vulnerability estimators for risk assessments of water resources systems, Hydrological Sciences Journal, 49, 755-767, 2004.

Klemes, V., Srikanthan, R., and McMahon, T. A.: Long-memory flow models in reservoir analysis: What is their practical value?, Water Resources Research, 17, 737-751, 1981.

Lence, B. J., Furst, J., and Matheson, S.: Distributive fairness as a criterion for sustainability evaluative measures and application to project selection, International Journal of Sustainable Development and World Ecology, 4, 245-258, 1997.

Loucks, D. P., and van Beek, E.: Water resources systems planning and management: An introduction to methods, models and applications, United Nations Educational, Scientific and Cultural Organization (UNESCO), Paris, 2005.

Loucks, D. P.: Quantifying trends in system sustainability, Hydrological Sciences Journal, 42, 513-530, 1997.

McMahon, T. A., Adeloye, A. J., and Sen-Lin, Z.: Understanding performance measures of reservoirs, Journal of Hydrology (Amsterdam), 324, 359-382, 2006.

Mendoza, V. M., Villanuave, E. E., and Adem, J.: Vulnerability of basins and watersheds in Mexico to global climate change, Climate Research, 9, 139-145, 1997.

Mishra, A. K., and Singh, V. P.: A review of drought concepts, Journal of Hydrology, 391, 202-216, 2010.

Moy, W. S., Cohon, J. L., and Revelle, C. S.: A programming model for analysis of reliability, resilience and vulnerability of a water supply reservoir, Water Resources Research, 22, 489-498, 1986.

National Science Council of Taiwan: Taiwan Climate Change Projection and Information Platform Project (TCCIP), 2010.

Palmer, W. C.: Meteorological drought, Research Paper 45, Weather Bureau, U.S. Dept. of Commerce, Washington, DC, 1965.

Ray, P. A., Vogel, R. M., and Watkins, D. W.: Robust optimization using a variety of performance indices, World Environmental and Water Resources Congress, ASCE,Providence, R.I., May 16-20, 2010.

Richardson, C. W.: Stochastic simulation of daily precipitation, temperature, and solar-radiation, Water Resources Research, 17, 182-190, 1981.

Sandoval-Solis, S., McKinney, D., and Loucks, D.: Sustainability index for water resources planning and management, Journal of Water Resources Planning and Management, 137, 381-390, 2011.

Schilling, J., Freier, K. P., Hertig, E., and Scheffran, J.: Climate change, vulnerability and adaptation in North Africa with focus on Morocco, Agriculture, Ecosystems and Environment, 156, 12-26, 2012.

Schubert, S.: A weather generator based on the European 'Grosswetterlagen', Climate Research, 4, 191-202, 1994.

Selker, J. S., and Haith, D. A.: Development and testing of single-parameter precipitation distributions, Water Resources Research, 26, 2733-2740, 1990.

Takeuchi, K., Hamlin, M., Kundzewicz, Z. W., Rosbjerg, D., and Simonovic, S. P.: Sustainable reservoir development and management, International Association of Hydrological Sciences, IAHS Publication no. 251, 1998.

Tseng, H. W., Yang, T. C., Kuo, C. M., and Yu, P. S.: Application of multi-site weather generators for investigating wet and dry spell lengths under climate change: A case study in Southern Taiwan, Water Resources Management, (in press), 2012.

Tung, C. P., and Haith, D. A.: Global-warming effects on New York streamflows, Journal of Water Resources Planning and Management, 121, 216-225, 1995.

Vano, J. A., Voisin, N., Cuo, L., Hamlet, A. F., Elsner, M. M., Palmer, R. N., Polebitski, A., and Lettenmaier, D. P.: Climate change impacts on water management in the Puget Sound region,Washington State, USA, Climatic Change, 102, 261-286, 2010.

Woolhiser, D. A., and Pegram, G. G. S.: Maximum likelihood estimation of fourier coefficients to describe seasonal variation of parameters in stochastic daily precipitation models, Journal of Applied Meteorology, 18, 34-42, 1979.

Woolhiser, D. A., and Roldan, J.: Seasonal and regional variability of parameters for stochastic daily precipitation models, Water Resources Research, 22, 965-978, 1986.

Woolhiser, D. A., and Roldan, J.: Stochastic daily precipitation models, 2. A comparison of distribution of amounts, Water Resources Research, 18, 1461-1468, 1982.

Yu, P. S., and Yang, T. C.: Fuzzy multi-objective function for rainfall-runoff model calibration, Journal of Hydrology, 238, 1-14, 2000.

Yu, P. S., Kuo, C. C., Leu, J. M., and Sung, C. W.: The influence of climate change on meteorological drought characteristic in Taiwan, Conference on Water Observation and Information System for Decision Support, Ohrid, FY Republic of Macedonia. 25-29 May, 2004.

Yu, P. S., Tseng, H. W., and Chen, S. T.: Impact of climate change on agriculture water resources for paddy rice over southern Taiwan, International Congress on Environmental Modelling and Software, Ottawa, Ontario, Canada. 5-8 July, 2010.

Yu, P. S., Yang, T. C., and Kuo, C. C.: Evaluating long-term trends in annual and seasonal precipitation in Taiwan, Water Resources Management, 20, 1007-1023, 2006.

Yu, P. S., Yang, T. C., and Wu, C. K.: Impact of climate change on water resources in southern Taiwan, Journal of Hydrology, 260, 161-175, 2002.

Zongxue, X., Jinno, K., Kawanura, A., Takesaki, S., and Ito, K.: Performance risk analysis for Fukuoka water supply system, Water Resources Management, 12, 13-30, 1998.

Table 1. Summary of selected GCMs in this study

Model	Country	Center	Resolution
CGCM3.1(T63)	Canada	CCCma	T63, L31
CSIRO-Mk3.5	Australia	CSIRO	T63, L18
ECHAM5/MPI-OM	Germany	MPI-M	T63, L31
GFDL-CM2.0	USA	GFDL	2.0°×2.5°, L24
GFDL-CM2.1	USA	GFDL	2.0°×2.5°, L24
MIROC3.2(hires)	Japan	NIES	T106, L56
MRI-CGCM2.3.2	Japan	MRI	T42, L30

Note: T stands for a horizontal resolution expression using triangular spectral truncation; T42, T63 and T106 are roughly equal to 2.8°×2.8°, 1.9°×1.9° and 1.1°×1.1°, respectively; L stands for a vertical resolution expression which is the number of vertical levels.

Table 2. Change rates (%) of monthly rainfall from the baseline period to the future period for different GCMs

GCM	Jan	Feb	Mar	Apr	May	Jun	Jul	Aug	Sep	Oct	Nov	Dec
CGCM3.1(T63)	-13.53	40.67	-4.26	-12.92	8.27	-18.13	-18.98	-2.34	18.14	-17.81	-31.99	-22.35
CSIRO-Mk3.5	-30.99	-21.97	-16.76	-10.28	-9.48	21.34	4.87	2.76	19.91	57.34	25.99	-23.24
ECHAM5/MPI-OM	9.67	-17.94	-12.82	25.39	3.80	5.94	-24.52	-35.88	2.52	-21.81	-15.21	19.29
GFDL-CM2.0	-6.87	2.80	-4.57	-7.80	-20.09	19.03	-17.17	-6.49	20.69	1.93	2.18	-0.49
GFDL-CM2.1	50.39	-36.44	-21.03	-6.00	-10.77	16.99	34.58	12.23	-32.54	-55.42	56.81	-5.56
MIROC3.2(hires)	0.80	13.20	-36.33	-33.01	-27.60	8.10	-1.13	-15.19	12.94	39.70	-23.24	10.22
MRI-CGCM2.3.2	-18.01	-52.24	-38.00	-1.54	15.64	3.77	30.95	13.89	18.65	-8.44	-46.89	-31.65

Table 3. Changes of monthly mean temperature (^{o}C) from the baseline period to the future period for different GCMs

GCM	Jan	Feb	Mar	Apr	May	Jun	Jul	Aug	Sep	Oct	Nov	Dec
CGCM3.1(T63)	0.70	0.64	0.98	1.61	1.29	1.44	1.45	1.40	1.66	1.34	1.44	1.07
CSIRO-Mk3.5	0.22	0.75	1.25	0.97	1.66	1.38	1.15	1.17	1.30	1.23	1.20	0.48
ECHAM5/MPI-OM	1.25	0.46	0.68	0.90	0.94	0.62	1.23	1.04	1.03	0.56	1.20	1.34
GFDL-CM2.0	0.99	1.13	0.81	0.50	0.72	0.66	1.38	1.03	0.99	0.47	0.77	1.30
GFDL-CM2.1	1.52	0.50	0.79	0.90	1.02	1.08	1.21	0.93	1.09	1.18	1.56	0.80
MIROC3.2(hires)	1.45	1.24	1.03	1.53	1.70	1.55	1.62	1.63	1.55	1.42	1.41	1.56
MRI-CGCM2.3.2	0.38	1.08	0.85	0.85	1.16	1.21	0.97	0.83	0.93	0.79	0.70	0.47

Table 4. Comparison of statistics for observed and generated daily rainfalls and temperatures

Daily Rainfall (unit: mm/day)						
Month	Mean		Standard Deviation		Skewness	
	Obs	Gen	Obs	Gen	Obs	Gen
1	4.53	4.63	8.54	8.06	4.72	3.56
2	7.25	7.19	12.32	12.51	3.61	4.33
3	7.97	8.72	14.68	15.99	3.76	4.54
4	9.37	8.84	15.39	14.70	2.78	4.79
5	15.44	16.35	25.00	25.02	3.19	3.44
6	19.27	19.03	32.26	31.36	3.48	3.74
7	17.82	18.29	43.35	43.79	6.99	7.77
8	21.12	22.62	45.39	47.56	5.93	5.51
9	13.51	14.95	36.41	38.34	8.51	9.35
10	5.18	5.21	11.46	11.05	5.80	6.32
11	2.72	2.85	5.54	6.20	3.87	6.27
12	4.26	4.66	7.05	7.51	2.71	3.92

Daily Temperature (unit: ^{o}C)						
Month	Mean		Standard Deviation		Skewness	
	Obs	Gen	Obs	Gen	Obs	Gen
1	12.45	12.39	2.34	2.28	-0.16	0.00
2	13.22	13.25	2.29	2.27	-0.33	-0.01
3	15.84	15.81	2.65	2.45	-0.93	0.02
4	18.07	18.09	1.97	1.92	-0.76	-0.06
5	19.73	19.70	1.28	1.26	-0.40	0.06
6	21.09	21.05	1.14	1.08	-0.71	-0.01
7	21.47	21.48	0.88	0.86	-0.95	-0.05
8	21.19	21.21	0.86	0.86	-0.73	-0.01
9	20.59	20.62	1.00	0.97	-0.53	-0.02
10	19.27	19.23	1.27	1.24	-0.71	-0.05
11	16.83	16.81	1.97	1.84	-0.58	0.05
12	13.55	13.64	2.39	2.29	-0.19	-0.02

Note: “Obs”and “Gen” are the abbreviations of “observed” and “generated” data, respectively.

Table 5. Comparison of statistics for observed and generated rainfalls at both monthly and yearly scales

Monthly Rainfalls (unit: mm/month)						
Month	Mean		Standard Deviation		Skewness	
	Obs	Gen	Obs	Gen	Obs	Gen
1	35.35	36.06	27.96	28.83	0.95	0.88
2	75.78	83.12	84.50	60.07	1.55	1.13
3	88.88	91.99	81.35	64.37	1.63	0.74
4	134.91	122.28	112.91	75.51	1.55	1.48
5	318.12	337.27	149.69	136.13	0.16	0.57
6	434.61	421.61	235.41	194.16	0.09	0.58
7	441.97	433.74	298.57	235.82	0.26	0.84
8	570.15	597.71	293.73	275.64	0.56	1.19
9	303.93	310.73	259.30	213.29	2.12	2.33
10	70.72	66.58	82.22	49.95	3.50	2.28
11	17.00	20.22	19.46	19.60	1.44	1.72
12	24.49	28.28	21.51	26.56	0.76	1.49

Yearly Rainfalls (unit: mm/year)					
Mean		Standard Deviation		Skewness	
Obs	Gen	Obs	Gen	Obs	Gen
2515.88	2549.58	695.82	489.09	0.18	0.37

Note: “Obs”and “Gen” are the abbreviations of “observed” and “generated” data, respectively.

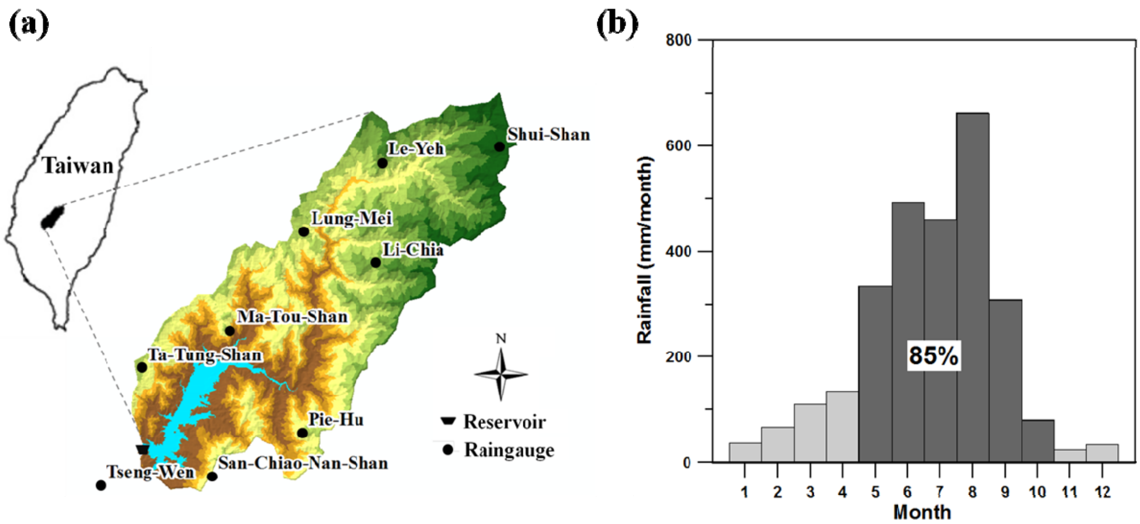

Figure 1. (a) The catchment of Tsengwen Reservoir and (b) mean monthly rainfalls

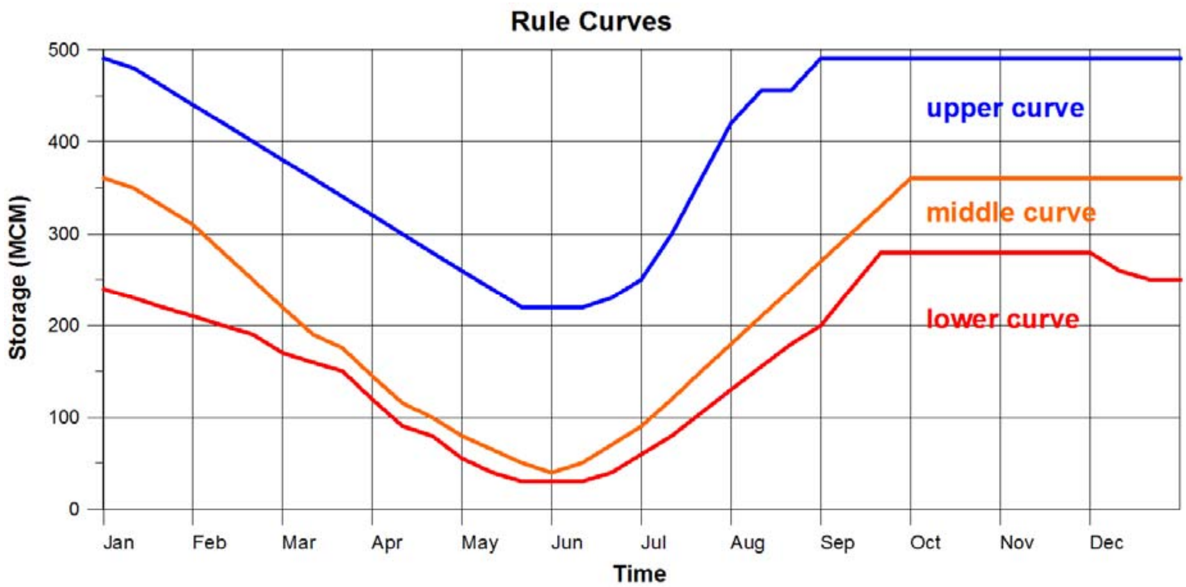

Figure 2. The rule curves of Tsengwen Reservoir

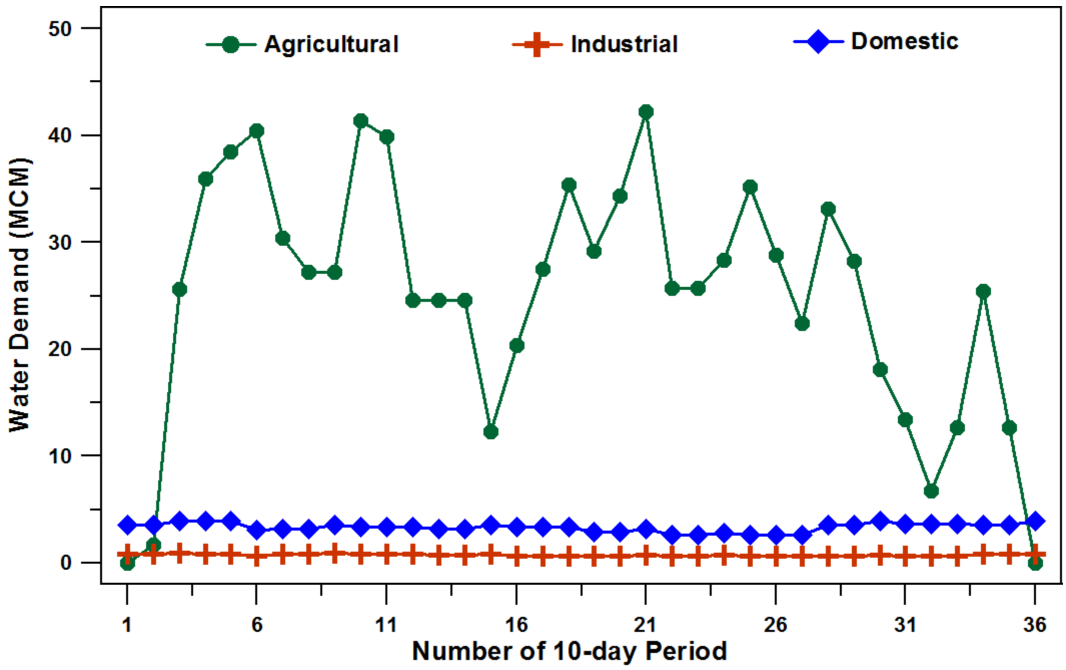

Figure 3. Demands of agricultural, industrial, and domestic water uses.

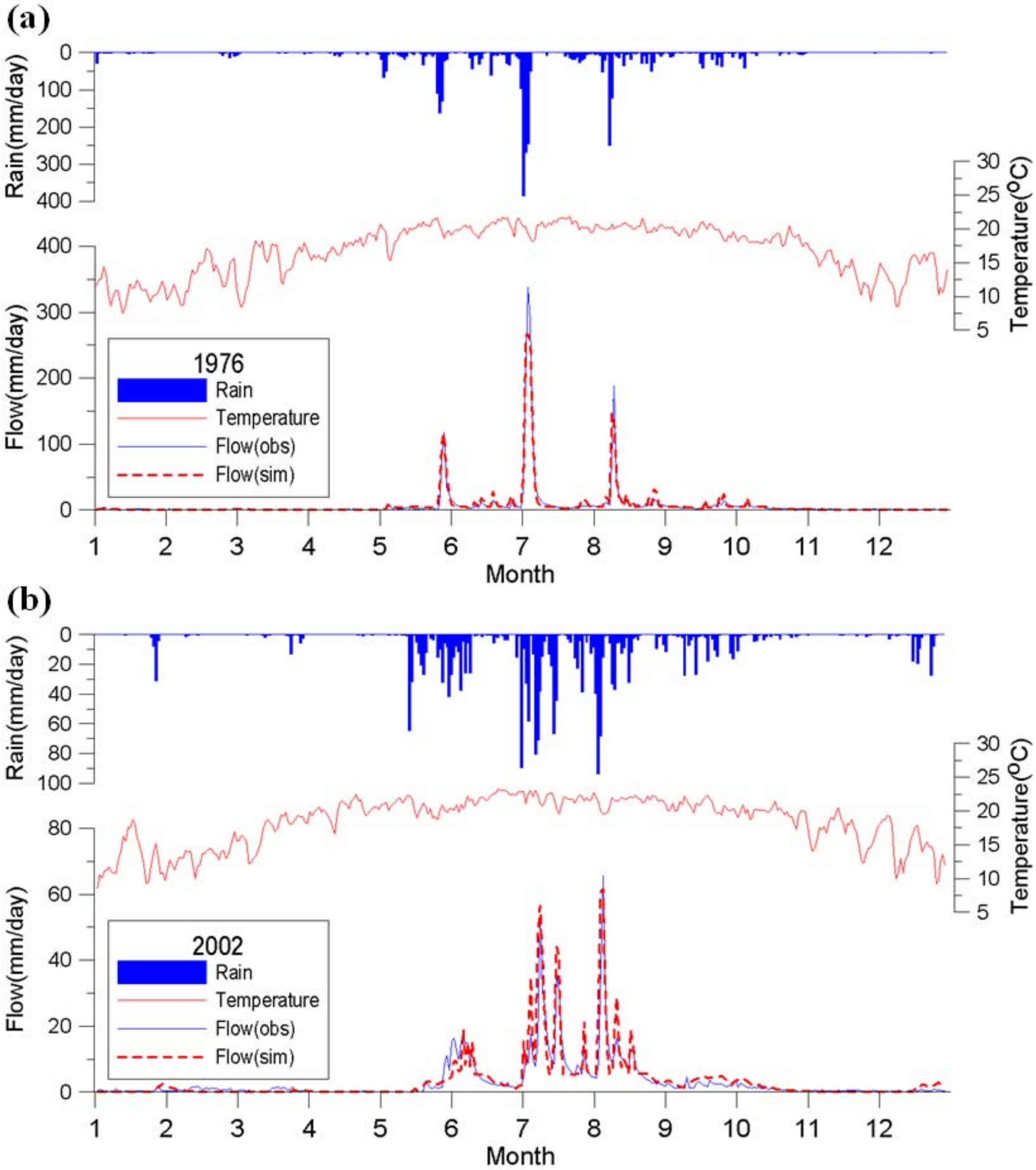

Figure 4. (a) Calibration and (b) verification results for the HBV-based hydrological model in 1976 and 2002, respectively.

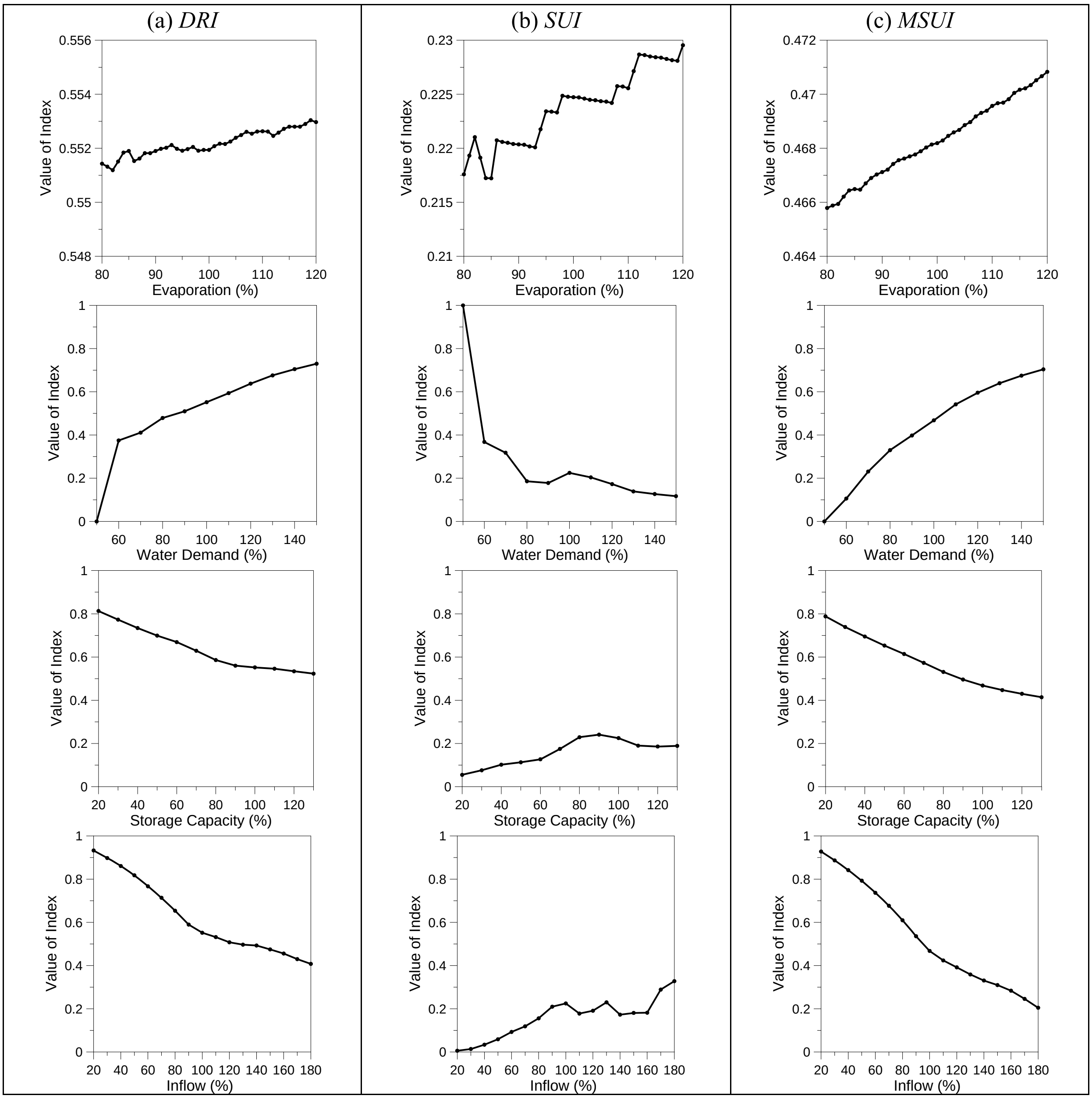

Figure 5. Analysis results of monotonic behavior for each index

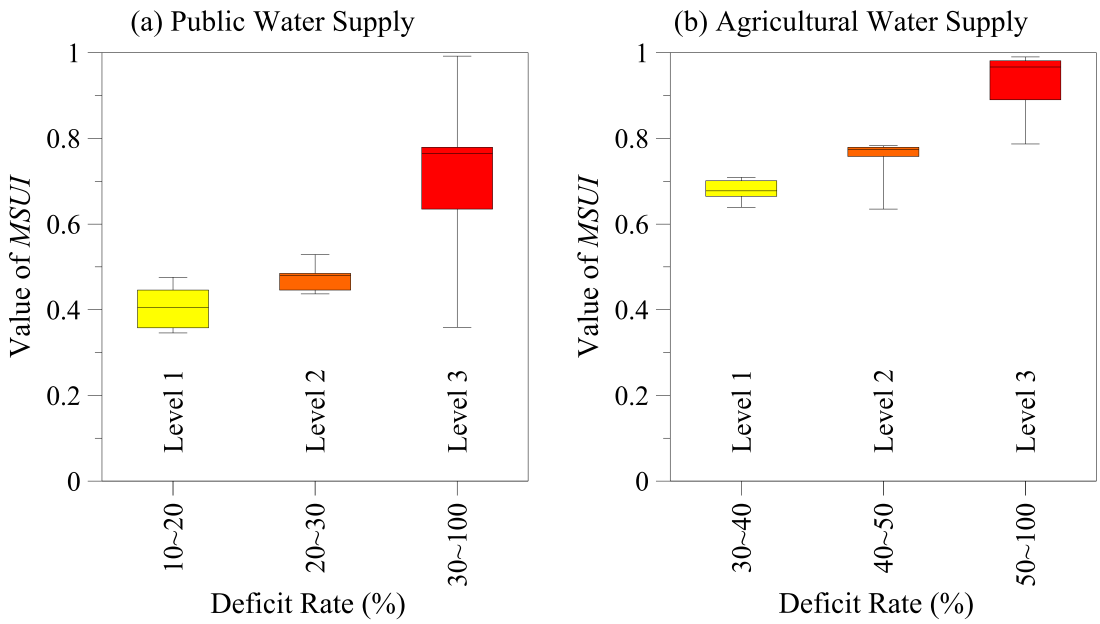

Figure 6. Box plots of *MSUI* value for each drought level

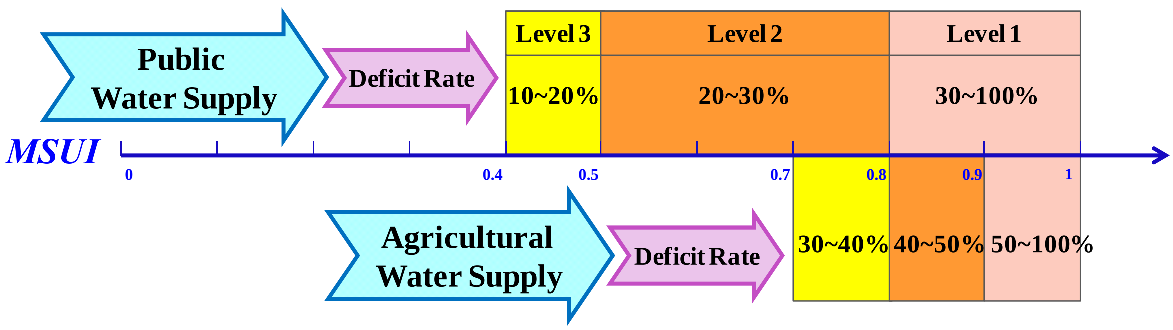

Figure 7. Drought levels and their corresponding *MSUI* values and deficit rates

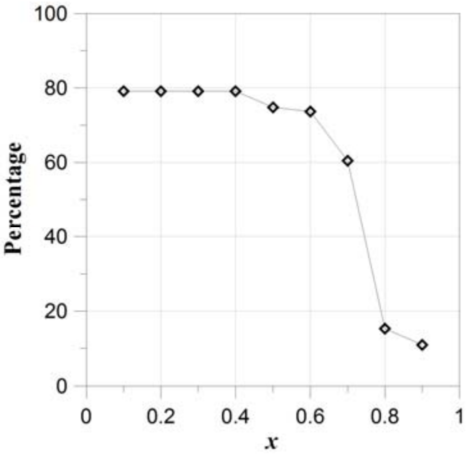

Figure 8. Percentage of the 10-day number with $MSUI \geq x$ to the 10-day number of historical drought. For example, 80% and 15% of the MSUI values are equal to or greater than 0.4 and 0.8, respectively. The drop between MSUI = 0.6 and 0.8 is very sharp.

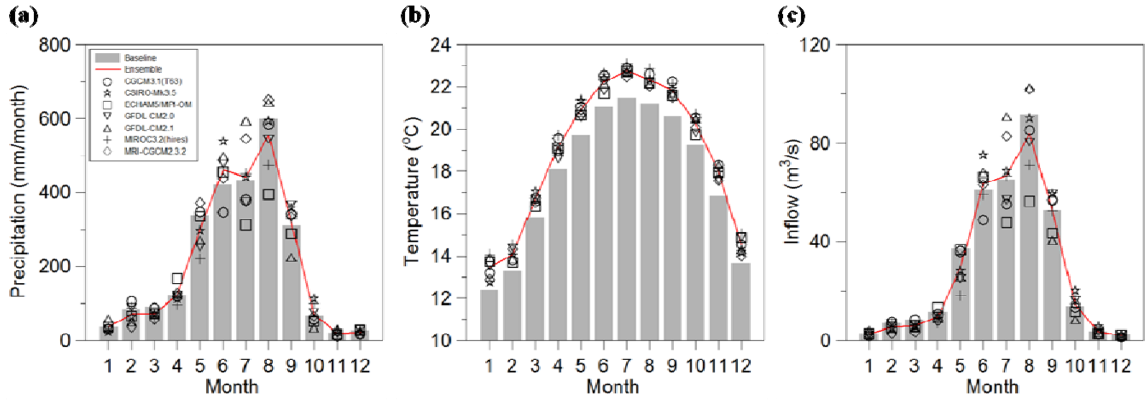

Figure 9. Projected (a) mean monthly rainfalls, (b) average monthly mean temperatures and (c) average monthly mean inflows by using different GCMs

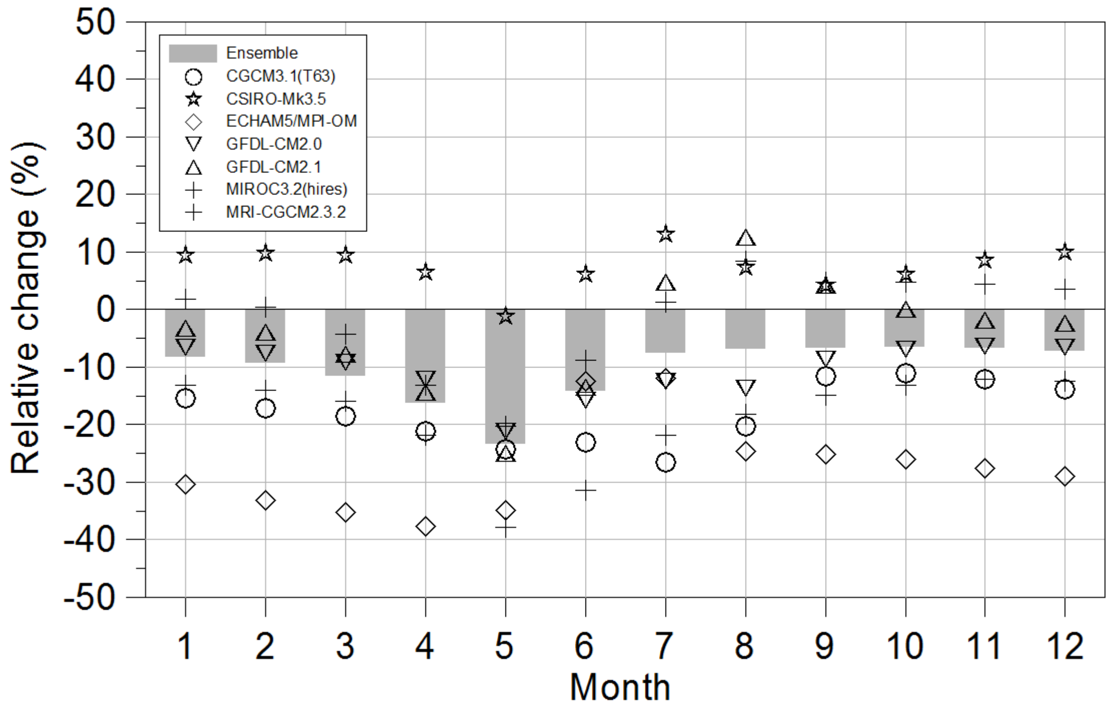

Figure 10. Percentage changes of mean monthly storage from the baseline period to the future period

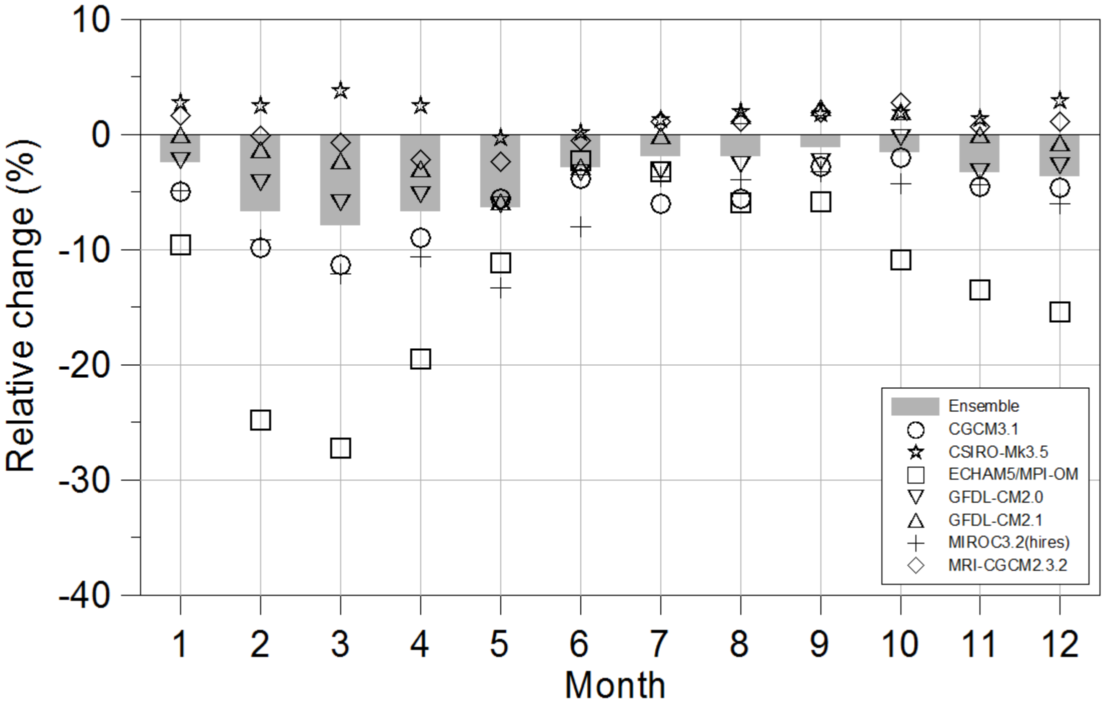

Figure 11. Percentage changes of mean monthly water supply amount from the baseline period to the future period

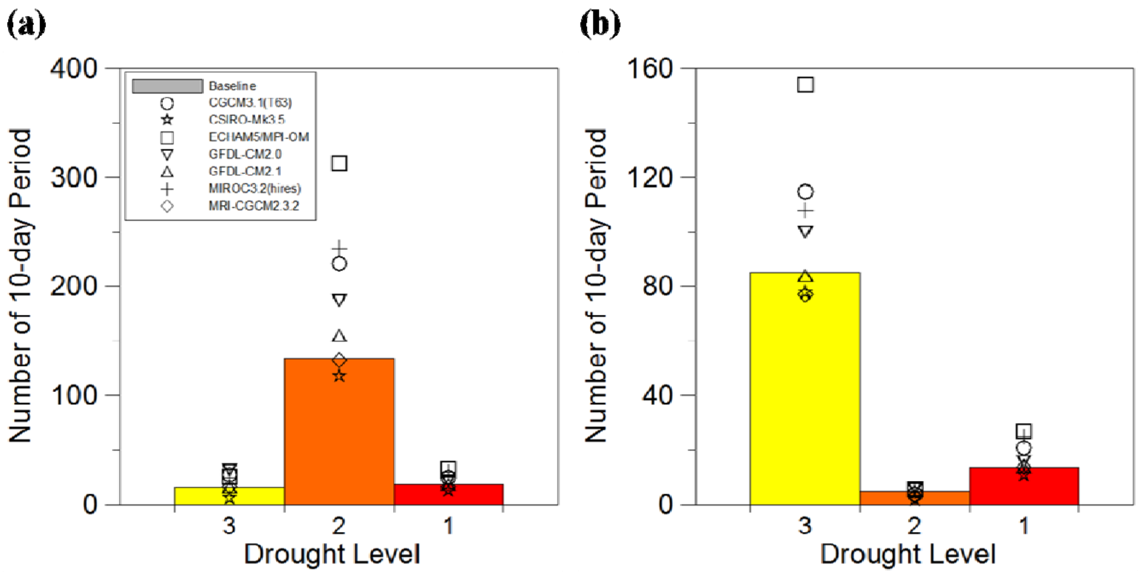

Figure 12. Numbers of 10-day period for different drought levels by using different GCMs for (a) public water supply and (b) agricultural water supply